

# Simplified test bench for experimental investigations of space heating appliances

N Paulus<sup>1,\*</sup> and V Lemort<sup>1</sup>

<sup>1</sup>University of Liège, Thermodynamics Laboratory, Allée de la découverte 17, Liège, Belgium

\* Email: nicolas.paulus@uliege.be

**Abstract.** The energy transition requires efficient space heating appliances. In that context, it is common that thermodynamics laboratories are asked to conduct experimental investigations on those appliances to establish or verify their performance. This paper aims to offer and report an example of a very simple test rig that allows for controlling both the space heating water flow rate and the space heating return temperature. Space heating depart temperature thus depends on those two controlled parameters as well as the heat transfer rate provided by the space heating appliance, based on its settings. The test rig described in this paper has been used to conduct experimental studies on residential Solid Oxide Fuel Cells used as micro-cogeneration units. It has the advantage of being reproducible or reused with other residential space heating appliances. It can easily be adapted for refrigeration appliances testing or even heat exchanger characterization. Also, the test rig controlling the space heating flow rate and working temperature implies an approximative cost of only about 1 k€ (with 2021 hardware prices, without the space heating appliance to be tested).

## 1. Introduction

Targets of temperature increase compared to pre-industrial levels have scientifically been linked to remaining carbon budgets of future Greenhouse Gases (GHG) emissions allowed for all humanity [1]. Actually, in its Sixth Assessment Report (AR6) released in early 2022, Intergovernmental Panel on Climate Change's Working Group III (IPCC WGIII) has reported that if humanity does not exceed 890 GtCO<sub>2</sub> of emissions from January 1st 2020, it will have 2 out of 3 chances of not exceeding the +2°C maximum limit set in the 'Paris Agreement' back in 2015 [2]. Mitigating GHG emissions is generally associated to the 'low carbon transition' [3], i.e. to the 'energy transition'.

Beside lowering the energy demand, i.e. the 'energy sobriety principle' [4], and increasing territorial carbon absorption [5], it is usually considered that one main pillar of the much-needed energy transition lies in the 'energy efficiency' [4]. Efficiency is always crucial at all levels, both in case of fossil fuel and renewable energy use. For space heating appliances at residential scale, energy efficiency and performance establishment or enhancement usually require specific laboratory investigations, with specific hardware.

This paper describes a simple test rig that has been used to conduct experimental studies on a residential Solid Oxide Fuel Cell (SOFC) used as a micro-cogeneration unit. The test rig offers the possibility of modulating independently the space heating water flow rate as well as the operating temperatures, by controlling the return temperature by means of a thermostatic 3-way valve such as the

one reported later on in figure 1(a). Space heating depart temperature thus depends on those two controlled parameters as well as the heat transfer rate provided by the space heating appliance, based on its settings (such as the power output setting), which by the way also depends on the two fore-mentioned controlled parameters.

Indeed, the purpose of the laboratory study, for which the test rig presented in this paper has been implemented, was to evaluate the heat recovery capacity of the fuel cell system, as well as establishing electrical and thermal efficiencies, according to the power output setting of the system.

The test rig described in this paper has the advantage of being reused or reproduced and adapted in order to evaluate the performance and efficiencies of other space heating appliances.

## 2. Test rig working principle

In practice, the heat recovery capacity of the tested fuel cell is mainly affected by the efficiency of the internal heat exchanger within the space heating appliance (that, in the case of the studied fuel cell system, recovers heat from the flue gases to the recovery heat circuit). This internal exchanger is shown in the test bench schematics of figure 2.

Therefore, the idea behind the laboratory test campaign was to evaluate this heat exchanger performance (for several fuel cell electrical output power settings). Considering that the heat-transfer fluid of the heat recovery circuit does not change (in most space heating applications, it is simple water), the heat-transfer is affected by the flow rate  $\dot{m}_A$  and the working temperatures (depart temperature  $T_D$  and return temperature  $T_R$ ). Indeed, the rate of recovered heat  $\dot{Q}_A$  (expressed as a power) is established through equation (1), i.e. the first thermodynamics law :

$$\dot{Q}_A(T_R, \dot{m}_A, \text{internal settings}) = \dot{m}_A c p_A (T_D - T_R) \quad (1)$$

Where  $c p_A$  is the specific heat capacity of the recovery water. In equation (1), depart temperature  $T_D$  is defined by the space heating appliance heat rate capability  $\dot{Q}_A$  at the given operating temperature, flow rate conditions and internal settings (mainly power modulation).

For some applications where the space heating depart temperature  $T_D$  (such as conventional gas condensing boilers) is a direct setpoint of the space heating appliance, equation (1) can be updated as in equation (2).

$$\dot{Q}_A = \dot{m}_A c p_A [T_D(\text{internal settings}) - T_R] \quad (2)$$

## 3. Detailed description of the test rig

The space heating heat rate  $\dot{Q}_A$  from equation (1), provided by the tested appliance, must trivially be dissipated by the test bench (at least for steady-state operating conditions to be reached). The base principle of the return temperature modulation consists in controlling the bypass of a high-capacity heat exchanger (fed with fresh or cooling water) thanks to a specific thermostatic 3-way valve (which has been presented in figure 1(a) and constitutes the key element of the test rig). This valve is currently manual but could easily be automated with a servomotor.

It has been chosen to allow the passive control of the temperature at its outlet between 20-55°C, which corresponds to the usual working temperature of the studied space heating appliance. Temperature control is based on the 'automated' mixture of hot and cold stream allowed by the thermostatic element within the valve. The hot stream is connected to the depart of the heating appliance whereas the cold stream is connected to the output of the high-capacity heat exchanger. This is a robust solution if the auxiliary fresh water flow rate or its temperature changes (change in the heat exchanger capability).

The high-capacity of the heat exchanger is provided by means of a connection to the water main (allowing a high flow rate auxiliary cooling water), as shown in figure 2. The specifications of the heat exchanger have no particular relevance as long as it allows a sufficient cooling capacity (with the auxiliary water from the mains). Unfortunately, this auxiliary water is currently directed to the sewers and not yet recuperated.

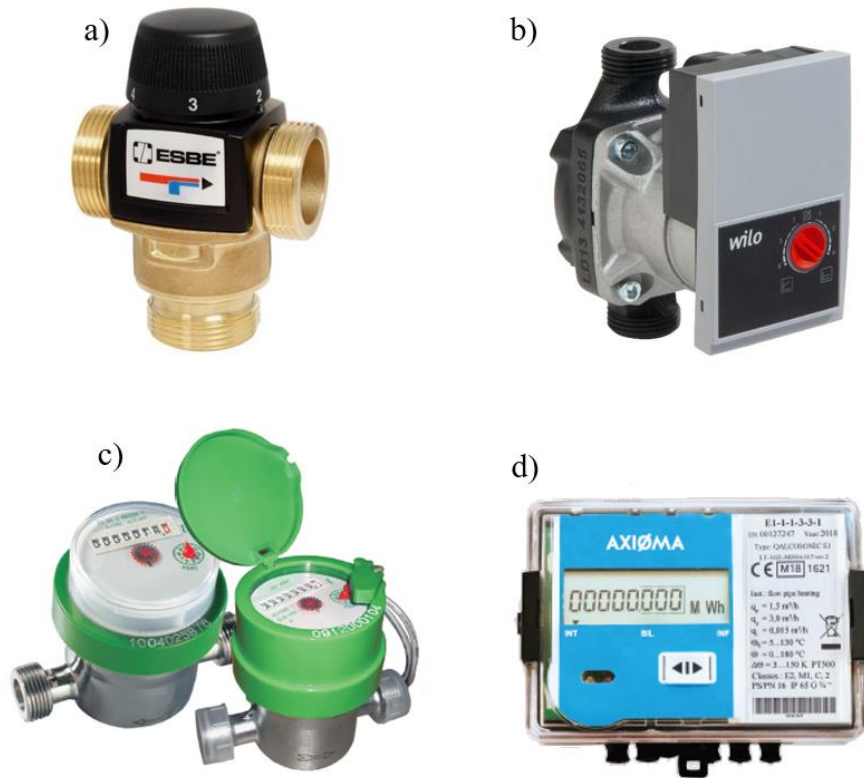


**Figure 1.** Specific elements used in the presented test-tig. a) Thermostatic 3-way valve to control the return temperature ('VTA 572' by ESBE). b) Variable speed circulator used in the laboratory test bench to control the space heating flow rate ('Yonos Para 15/6' by Wilo). c) Volumetric watermeter used to measure space heating flow rate  $\dot{m}_A$  ('DHV1300' by DH Metering Europe). d) Optional ultrasonic heat meter included in the test-bench that allows for directly measuring space heating heat transfer ('Qalcosonic E1' by Axioma)

The test bench schematics used to test a residential micro-generation Solid Oxide Fuel Cell (SOFC) is presented in figure 2. This particular fuel cell system is fed with natural gas and requires fresh water (that it filters) for steam reforming purposes. It rejects potential water excess from condensate recuperation in the exhaust and from its internal water reverse-osmosis filters [6]. This explains the need for gas meters, exhaust doubled-walled chimney (oxygen required for the fuel cell reaction comes from external ambient air). The fuel cell system's output power is DC and requires an inverter in order to reject electric on the grid, also explaining the need for electric meters. A passive deaerator is used as advised by the Fuel Cell manufacturer in order to remove gases, mainly oxygen (that can cause corrosion damage) from the space heating circuits [7]. The facilities of the fuel cell test bench described in this paper are shown in figure 3.

The part that is specifically relevant to this paper (that allows for controlling working temperatures and space heating water flow rate) is the one on the left of figure 2 (squared in blue).

Water flow rate  $\dot{m}_A$  is simply set by adjusting the power output of the heat recovery variable-speed circulator (presented in figure 2).

Since the internal elements of the thermostatic 3-way valve will induce a pressure drop in the space heat circuit (in both hydraulic lines of the 3-way mixing valve), it will have an impact on the space heating flow rate  $\dot{m}_A$ . This pressure drop change can be compensated by adjusting the speed of the circulator but since it is a rotative manual button, observable in figure 1(b), its resolution, which is highly sensitive, might not suffice. Therefore, a combination of parallel manual 2-way valves (including a sensitive needle valve) has been implemented on the recovery circuit. This 'pressure drop manual regulator' apparatus is shown in figure 2.

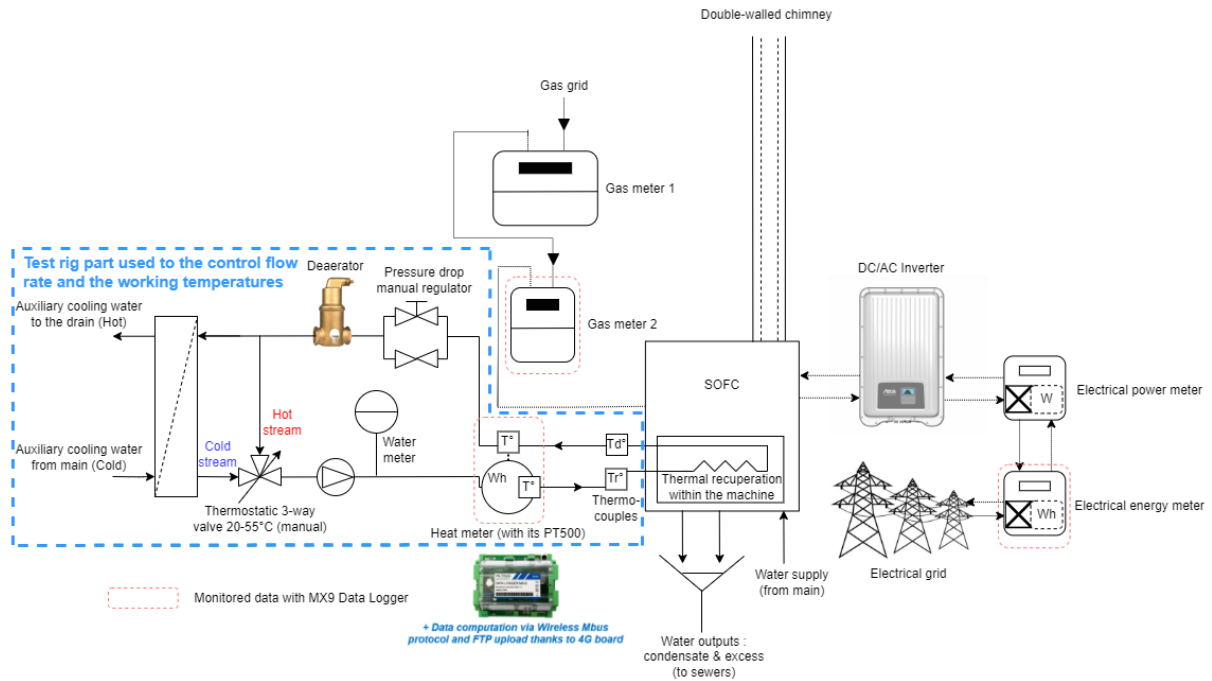


**Figure 2.** Schematics of the Fuel Cell test bench described in this paper



**Figure 3.** Photographs of the Fuel Cell test bench described in this paper

It is worth mentioning that the thermostatic 3-way valve that controls the return temperature  $T_R$  could be placed both at the inlet ('recirculation' configuration) or at the outlet ('bypass' configuration) of the high-capacity dissipating heat exchanger, as illustrated in figure 4. However, the 'recirculation' configuration of figure 4(b) is not ideal for two main reasons:

- It requires the variable-speed circulator that is supposed to control the space heating flow rate  $\dot{m}_A$  to be placed after the 3-way valve. Indeed, if it was placed on the main line (connected to

the studied space-heating appliance), its flow could be stopped if the 3-way valve was set to completely block the hot stream inlet (at the depart temperature  $T_D$ ) and recirculate all the flow in the heat exchanger. This could happen if the 3-way valve is set to low temperature outputs. With the variable-speed circulator placed after the 3-way valve, it does not directly ‘control’ the space heating flow rate  $\dot{m}_A$  as desired and even worse, if the 3-way valve is set to low temperature outputs and recirculate all the flow in the heat exchanger, the space heating flow rate  $\dot{m}_A$  could be reduced to zero.

- In addition, in the ‘recirculation’ configuration, the 3-way valve only controls the return temperature  $T_R$  as desired indirectly (it rather directly regulates the temperature at the inlet of the heat exchanger). The return temperature  $T_R$  indeed occurs at its cold stream inlet rather than at its outlet.

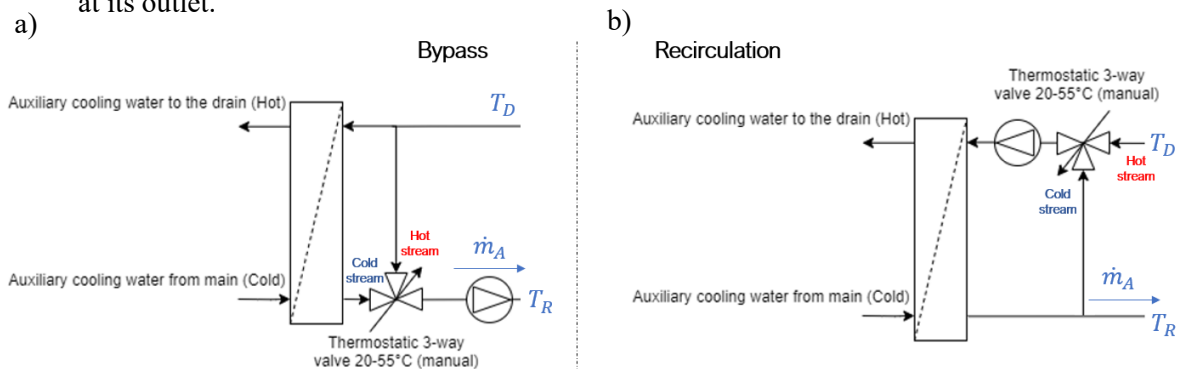


**Figure 4.** Two possibilities for placing the thermostatic 3-way valve that controls the return temperature  $T_R$  (the one on the left is the one implemented in the test rig described in this paper as it is the one that directly connects the output of the 3-way valve to the return of the space heating appliance, which temperature must be controlled)

On the fuel cell test bench, the space heating flow rate  $\dot{m}_A$  can be measured by means of a simple pulsed volumetric watermeter, such as the one shown in figure 1(c).

In the test-bench of figure 2, an optional heat meter has also been included, presented in figure 1(d). This allows for a direct measure of the space heating heat rate. In addition, that same sensor provides the space heating flow rate  $\dot{m}_A$ , depart temperature  $T_D$  and return temperature  $T_R$  (thanks to PT500 probes involved within the sensor, as illustrated in figure 2). It can be pointed out that this sensor has the ability to establish Wireless M-bus (Meter-bus) connection [8] so a ‘datalogger’ can be used to collect the measurements (as illustrated in figure 2). This particular sensor is known to be used in field-test monitoring studies [6, 9, 10, 11, 12].

Depart temperature  $T_D$  and return temperature  $T_R$  can easily be measured with ‘type T’ thermocouples, for instance.

It is worth mentioning that such a test bench configuration allows for imposing temperatures and/or space heating flow rate steps. It can simply be performed by turning the manual handle of the 3-way valve and/or of the variable speed circulator. Thus, in addition to the steady-state investigations that can be established as described earlier, this allows for transient testing. Similarly, the time-constant of the system can also be established.

For information and to illustrate the cost efficiency of such a test rig system, the total approximative costs (with prices valid for the year 2021) of the part of the test rig that allows for controlling working temperatures and space heating flow rate is provided in table 1.

**Table 1.** Cost estimate of the part of the test rig that allows for controlling working temperatures and space heating flow rate (total of about 1k€).

Hardware	Approximative price in 2021 (€)
Variable speed circulator ('Yonos Para 15/6' by Wilo)	250
Thermostatic 3-way valve ('VTA 572' by ESBE)	100
Volumetric watermeter ('DHV1300' by DH Metering Europe)	150
High-capacity heat exchanger (of any kind)	200
'Pressure drop manual regulator' (as in figure 2)	50
Connecting flexibles pipes and auxiliaries (such as thermocouples, deaerator, expansion valve, check valve)	250

#### 4. Potential outcomes : example of use of the test rig

As explained, the test rig described in this paper has been implemented in order to evaluate the performance of the heat recovery capacity of the tested fuel cell. Figure 5 is presented in this paper as an example of the possible outcomes of such a test rig. By measuring the recovery heat rate on the test rig (as explained) as well as by establishing the energy content of the volume of natural gas consumed by the fuel cell [13] (monitored thanks to a simple gas meter), thermal efficiencies can be established in any operating conditions.

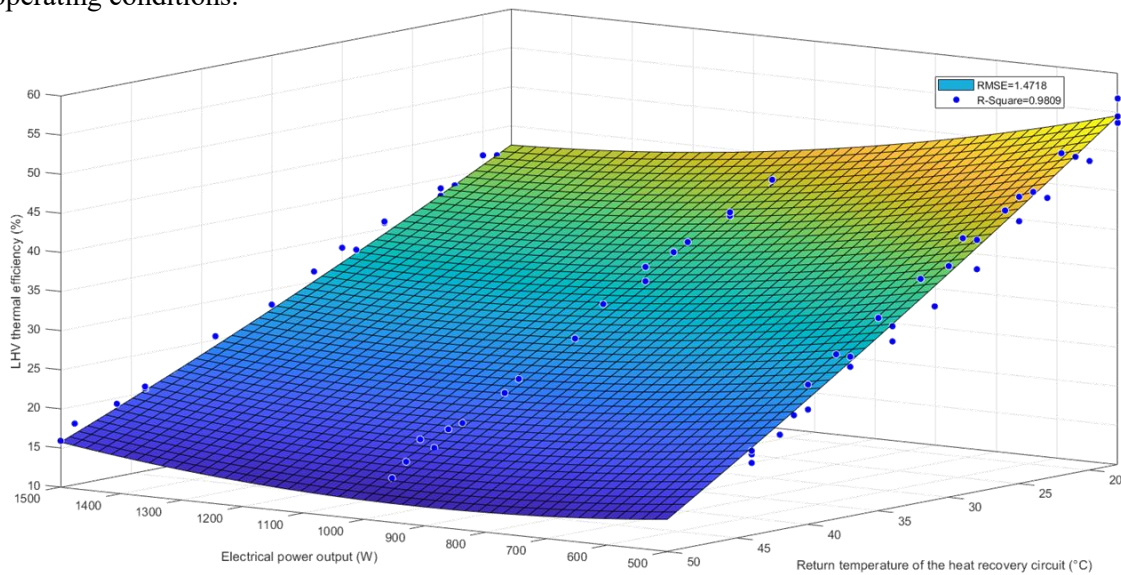


**Figure 5.** Low Heating Value (LHV) thermal efficiency experimental data and regressed thermal model of the studied fuel cell presented in this paper as an example of possible scientific outcomes achieved with the reported test rig. Dots correspond to the experimental data retrieved thanks to the reported test rig whereas the 3-D surface plot correspond to the (polynomial) regressed model of the fuel cell LHV thermal efficiency (based on the experimental dots).

In this case, the tested operating conditions (the inputs) are defined by the return temperature of the heat recovery circuit (controlled with the presented test rig) and the electrical power output of the fuel cell (not controlled by the test rig as it is a direct setting of the tested fuel cell). It is worth noting that the heat recovery flow rate (also controlled by the test rig) is not presented in figure 5 as it has been found to only have an insignificant impact on the thermal efficiency of the fuel cell.

For instance, thanks to the reported test-rig, figure 5 demonstrated that the maximum Low Heating Value (LHV) thermal efficiency of the tested fuel cell (close to 55%) is achieved at minimal electrical output power, i.e. 500 W<sub>el</sub> and at minimal working temperatures, i.e. return temperature about 20 °C. It can be pointed out that in those conditions, the heat recovery rate is about 700 W<sub>th</sub> and the electrical LHV efficiency is close to 40% (which are both not shown in figure 5). These operating conditions trivially lead to a quite tremendous total LHV efficiency close to 95% (= 55% + 40%).

Also, for information, it can be seen in figure 5 that the decrease in thermal efficiency is pretty much linear either to the increase in electrical power output or to the increase in working temperatures. It is worth mentioning that at higher electrical output power setting, the electrical LHV efficiency of the fuel cell increases (which is not shown in figure 5) and balances the LHV thermal efficiency decrease. Therefore, it cannot be simply established that the system shall only be used at its minimal electrical output (of 500 W<sub>el</sub>). Higher electrical efficiency is indeed sometimes preferable for some applications/households (with high electrical needs, such as the ones represented by the use of electric cars, for example).

However, it can still be established from figure 5 that, at any electrical power output, the lower the working temperature of the terminal units associated with the fuel cell, the higher the thermal efficiency. Therefore, households that have invested in such a fuel cell micro-cogeneration system that do not already use the heat recovered in any kind of underfloor heating or radiant walls and ceilings shall consider investing in fan coils and/or low temperature fan convectors [14].

## 5. Conclusions

This paper has demonstrated a very simple and affordable (about 1 k€ or less) space heating appliances test rig part. It allows for the modulation of the space heating flow rate and of the working temperatures respectively thanks to a variable speed circulator and a thermostatic 3-way valve. This latter is placed to bypass part of the space heating flow going to a high-capacity dissipating heat exchanger.

Also, temperatures and/or space heating flow rate steps can be easily implemented and studied with the proposed configuration. So, in addition to steady-state operating conditions, transient tests can be performed (for example, to study the time-constant of the system). For instance, this particular test rig configuration has been used for the experimental investigations of a residential micro-cogeneration of a Solid Oxide Fuel Cell.

It is worth mentioning that the proposed simple test rig configuration (based on a thermostatic 3-way valve) can be easily similarly reproduced for refrigeration appliances testing (or even heat exchanger characterization).

At last, a major improvement of the system would consist in the automatization of the elements currently used manually to control the operating conditions (without changing the base principle of the test bench). Indeed, the variable speed circulator could be replaced by one that offers a Pulse-width modulation (PWM) capability to control its rotating speed [15]. Also, the thermostatic 3-way valve handle could be mechanically associated to a servomotor. The variables used for their regulation would trivially be again the space heating flow rate and the return temperature.

Such an automated test rig could thus reproduce space heating demand profiles of typical households or dwellings. In its most advanced form, such a test rig could be used to implement a 'hardware in the loop' capability [16]. This would mean that the test rig would be associated to a software that simulate space heating demand profile based on a particular building's data (such as solar heat gain [17] or insulation levels) as well as based on weather data. This will allow for studying and experimentally verifying the relevance of the association of any studied space heating appliance with any building type and/or climatic region.

## Acknowledgements

The authors would like to acknowledge and thank the Gas.be ([www.gas.be](http://www.gas.be)) company for providing the Solid Oxide Fuel Cell used on the test rig described in this paper.

## References

- [1] J. Rogelj, P. M. Forster, E. Kriegler, C. J. Smith and R. Séférian, “Estimating and tracking the remaining carbon budget for stringent climate targets,” *Nature*, vol. 571, no. 7765, 2019.
- [2] N. Paulus, “Will Greenhouse Gas emission commitments in France and Wallonia respect IPCC’s carbon budget ?,” *Journal of Cleaner Production*, vol. Under review, 2022.
- [3] R. W. Wimbadi and R. Djalante, “From decarbonization to low carbon development and transition: A systematic literature review of the conceptualization of moving toward net-zero carbon dioxide emission (1995–2019),” *Journal of Cleaner Production*, vol. 256, 2020.
- [4] I. Campos and E. Marín-González, “People in transitions: Energy citizenship, prosumerism and social movements in Europe,” *Energy Research & Social Science*, vol. 69, 2020.
- [5] N. Paulus, “From 'equity' carbon budget to individual carbon footprint mitigation pathways : examples for Wallonia and France,” *Environmental Development*, vol. Under Review, 2022.
- [6] N. Paulus and V. Lemort, “Field-test performance of Solid Oxide Fuel Cells (SOFC) for residential cogeneration applications,” *Proceedings of the 7th International High Performance Buildings Conference at Purdue*, 2022. <https://docs.lib.purdue.edu/ihpbc/405/>
- [7] P. O’Kelly, “Deaerators and Feedwater Heaters,” in *Computer Simulation of Thermal Plant Operations*, New York, Springer, 2013.
- [8] EN13757-4, *Communication systems for meters and remote reading of meters - Part 4: Wireless meter readout (Radio meter reading for operation in SRD bands)*, European Commission, 2013.
- [9] N. Paulus and V. Lemort, “Correlation between field-test and laboratory results for a Proton Exchange Membrane Fuel Cell (PEMFC) used as a residential cogeneration system,” *Proceedings of the 30e Congrès de la Société Française de Thermique*, 2022. <https://doi.org/10.25855/SFT2022-119>
- [10] N. Paulus and V. Lemort, “Grid-impact factors of field-tested residential Proton Exchange Membrane Fuel Cell systems,” in *Proceedings of the 14th REHVA World Congress*, 2022. <https://doi.org/10.34641/clima.2022.176>
- [11] N. Paulus, C. Davila and V. Lemort, “Field-test economic and ecological performance of Proton Exchange Membrane Fuel Cells (PEMFC) used in micro-combined heat and power residential applications (micro-CHP),” *Proceedings of the 35th International Conference On Efficiency, Cost, Optimization, Simulation and Environmental Impact of Energy Systems*, 2022.
- [12] C. Davila, N. Paulus and V. Lemort, “Experimental Investigation of a Gas Driven Absorption Heat Pump and In-Situ Monitoring,” *Proceedings of the 9th Heat Powered Cycles International Conference (HPC 2021)*, 2022.
- [13] N. Paulus and V. Lemort, “Establishing the energy content of natural gas residential consumption : example with Belgian field-test applications,” *Proceedings of 8th Conference of the Sustainable Solutions for Energy and Environment*, 2022.
- [14] J. M.-P. Sala Lizarraga and A. Picallo-Perez, “Chapter 1 - Efficient buildings and the arguments for incorporating exergy,” in *Exergy Analysis and Thermoconomics of Buildings*, vol. 13, 2020.
- [15] A. Gagliano and S. Aneli, “Recent Advances in Renewable Energy Technologies,” in *Chapter 2 - Energy analysis of hybrid solar thermal plants (PV/T)*, Elsevier, 2021, pp. 45-90.
- [16] A. Tejada De La Cruz, P. Riviere, D. Marchio, O. Cauret and A. Milu, “Hardware in the loop test bench using Modelica: A platform to test and improve the control of heating systems,” *Applied Energy*, vol. 188, 2017.
- [17] G. Oliveti, N. Arcuri, R. Bruno and M. De Simone, “An accurate calculation model of solar heat gain through glazed surfaces,” *Energy and Buildings*, vol. 43, no. 2, 2011.